

**Auger recombination as the dominant nonradiative recombination channel in InN**YongJin Cho,<sup>\*</sup> Xiang Lue, Martin Wienold, Manfred Ramsteiner, Holger T. Grahn, and Oliver Brandt<sup>†</sup>  
*Paul-Drude-Institut für Festkörperelektronik, Hausvogteiplatz 5–7, 10117 Berlin, Germany*

(Received 1 March 2013; published 9 April 2013)

We investigate the dependence of the photoluminescence intensity of degenerately doped ( $6 \times 10^{17}$ - to  $1 \times 10^{20}$ - $\text{cm}^{-3}$ ) InN films on their threading dislocation density and background doping level. The photoluminescence intensity is found to be not determined by the structural quality of the film but by its doping density. The inverse relationship between the photoluminescence intensity and the electron density suggests that Auger recombination is the mechanism which actually limits the internal quantum efficiency of these films.

DOI: [10.1103/PhysRevB.87.155203](https://doi.org/10.1103/PhysRevB.87.155203)

PACS number(s): 79.20.Fv, 78.30.Fs, 78.55.Cr, 78.66.Fd

One of the most remarkable events, just a decade ago in the history of semiconductor research, has been the revision of the band gap of InN. Instead of the established value of 2 eV, data obtained on single-crystalline films fabricated by plasma-assisted molecular-beam epitaxy (PAMBE) implied a band gap as low as 0.8 eV (Refs. 1 and 2) with current values converging at 0.60 eV.<sup>3–5</sup> The reason for this unprecedented change from a wide- to a narrow-gap semiconductor is believed to be the high affinity of InN to O, resulting in a high concentration of O in InN on substitutional N sites.<sup>6</sup> For concentrations exceeding several percent, an In(O,N) alloy may form which is a semiconducting material with a band-gap opening with increasing O content towards the visible spectral range. For concentrations of O in the doping range, O acts as a shallow donor in InN, and the *apparent* band gap observed in transmission spectra is determined by the Burstein-Moss shift due to the high density of electrons in the conduction band.

All of these recent data stem from material prepared heteroepitaxially, primarily by PAMBE on foreign substrates, such as GaN or ZnO (Ref. 7) with a significant lattice mismatch. Consequently, all of these films exhibit high densities of threading dislocations. Regarding the structural quality of InN, little progress has been made over the past decades, but the advance in vacuum technology and source purity has been considerable as reflected by the steady decrease in the background doping level in InN. Indeed, state-of-the-art InN films now exhibit electron densities in the mid- $10^{17}$ - $\text{cm}^{-3}$  range.<sup>3</sup> Simultaneously, reports of room-temperature photoluminescence (PL) of InN have become widespread only after the revision of its band gap. This observation may suggest that the radiative recombination in today's InN films is actually not limited by nonradiative recombination due to defects but intrinsically by Auger recombination.<sup>8,9</sup> Such a result would not be surprising given the fact that Auger recombination limits the performance of infrared lasers fabricated from most semiconductors with a similarly narrow band gap.<sup>10–12</sup>

In this paper, we critically examine the influence of the threading dislocation density and the background doping level on the room-temperature PL intensity of InN films grown by PAMBE. We find that the PL intensity exhibits no correlation with the dislocation density but is inversely proportional to the background electron density  $n$ . We analyze the data quantitatively and deduce the Auger coefficient  $B_1$  for degenerate InN.

The unintentionally doped InN films presented here were directly grown on O-face ZnO(000 $\bar{1}$ ) substrates (InN/ZnO) by

PAMBE. The films under investigation have been grown at temperatures between 375 and 550 °C and exhibit thicknesses between 0.13 and 2.5  $\mu\text{m}$ . The electron density  $n$  in InN/ZnO has been found to increase drastically with increasing substrate temperature and with decreasing film thickness<sup>7</sup> because of an interfacial reaction and the resulting incorporation of O donors<sup>13,14</sup> in the InN film. For comparison, we fabricated two additional InN films. First, a 0.9- $\mu\text{m}$ -thick InN film grown at 500 °C onto a 0.5- $\mu\text{m}$ -thick GaN buffer on a sapphire substrate (InN/GaN/sapphire) and, second, an intentionally Si-doped 1.85- $\mu\text{m}$ -thick InN film grown on ZnO at 425 °C (InN:Si/ZnO). The structural quality of all these InN films was evaluated by x-ray diffraction (XRD)  $\omega$  scans across the (10 $\bar{1}$ 2) reflection in quasisymmetric geometry. The full width at half maximum (FWHM) of these scans is a reliable indicator for the total threading dislocation density in the film.<sup>7,15</sup> PL measurements at 300 K were performed using a Bruker IFS 120HR Fourier-transform infrared spectrometer equipped with an InSb detector. The measured PL spectra were corrected for the system response measured with a calibrated halogen lamp. Raman spectra at 300 K were recorded in a  $z(x, -)\bar{z}$  backscattering configuration using a HR-LabRAM spectrograph (HORIBA/Jobin-Yvon) equipped with a charge-coupled device detector. The PL and Raman spectra were excited at 643 and 632.8 nm, respectively, i.e., at essentially the same wavelength. Thus, the PL ( $1/\alpha$ ) and Raman ( $1/2\alpha$ ) probing depths are  $\approx 100$  and  $\approx 50$  nm based on the absorption coefficient  $\alpha$  measured by Kasic *et al.*<sup>16</sup> The electron density ( $n$ ) of the samples was estimated by the procedure described in Ref. 17.

Figure 1(a) shows the room-temperature PL spectra of three InN films with different thicknesses grown at 475 °C. The spectra exhibit the characteristic near-band-edge emission observed for degenerate InN films<sup>18–20</sup> and no deep-level emission down to photon energies of 0.35 eV. Their integrated PL intensities  $I_{\text{int}}$  and peak energies  $E_p$  are displayed in the inset of Fig. 1(a). With increasing film thickness,  $I_{\text{int}}$  increases by a factor of 3, and  $E_p$  decreases by 100 meV. Figure 1(b) shows the Raman spectra of the same samples. In addition to the  $E_2$  phonon peak of InN, the coupled plasmon/longitudinal-optical-phonon mode ( $L^-$ ) (Refs. 21–23) is observed in the frequency region of 420–440  $\text{cm}^{-1}$ . The frequency of this mode reflects the electron density.<sup>22–24</sup> The redshift observed with increasing thickness as indicated with the dotted line, thus, implies that  $n$  decreases with increasing film thickness, confirming our previous result.<sup>7</sup>

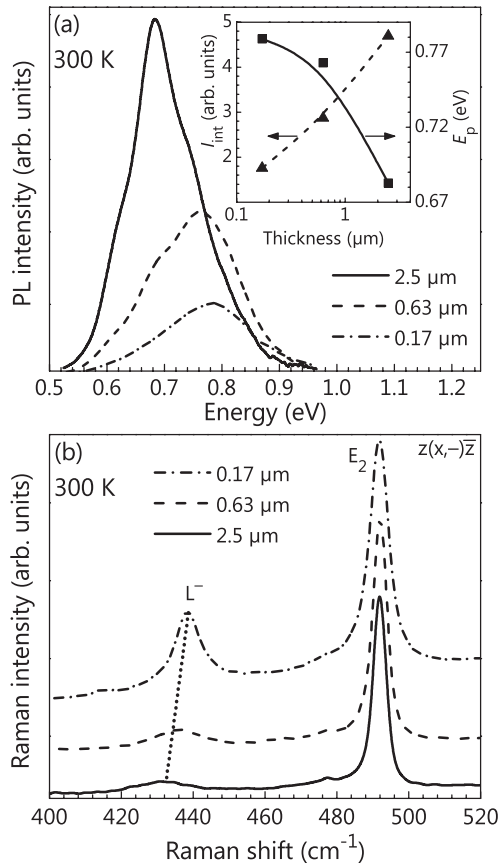


FIG. 1. Room-temperature (a) PL and (b) Raman spectra of InN films with different thicknesses as indicated grown at 475 °C. The Raman spectra are normalized to the intensity of the  $E_2$  peak and are vertically shifted for clarity. The inset in (a) shows the integrated PL intensity (triangles) and the PL peak energy (squares) of the InN films. The lines are guides to the eye.

The observed redshift in  $E_p$  with increasing thickness may, therefore, be attributed to a decreasing Burstein-Moss shift with decreasing  $n$ , which becomes observable in emission due to the existence of localized hole states.<sup>18</sup> It is tempting to conclude that the simultaneous increase in  $I_{\text{int}}$  is correlated to this decrease in  $n$  as well. However, the FWHM of our XRD  $\omega$  scans also monotonically decreases with increasing thickness. Specifically, we obtained for the 0.17-, 0.63-, and 2.5- $\mu\text{m}$ -thick InN films a FWHM of 0.56, 0.34, and 0.17°, respectively. One may, thus, argue that both the enhanced PL intensity and the redshift in  $E_p$  with increasing thickness may be due to an improved structural quality (i.e., a lower dislocation density) since threading dislocations have also been proposed to act as donors in InN.<sup>25,26</sup>

To address this potential relation between the dislocation density and the PL intensity of InN, we have characterized all InN films under investigation by XRD  $\omega$  scans. Figure 2(a) displays  $I_{\text{int}}$  vs the FWHM of these scans. Clearly, films with a low dislocation density do not necessarily exhibit a high PL intensity and vice versa. In particular, our control sample on a GaN-buffered sapphire substrate exhibits, as expected, a higher dislocation density than most of the InN/ZnO films but still a significant PL intensity. In other words, PL intensity and dislocation density do not seem to be correlated.

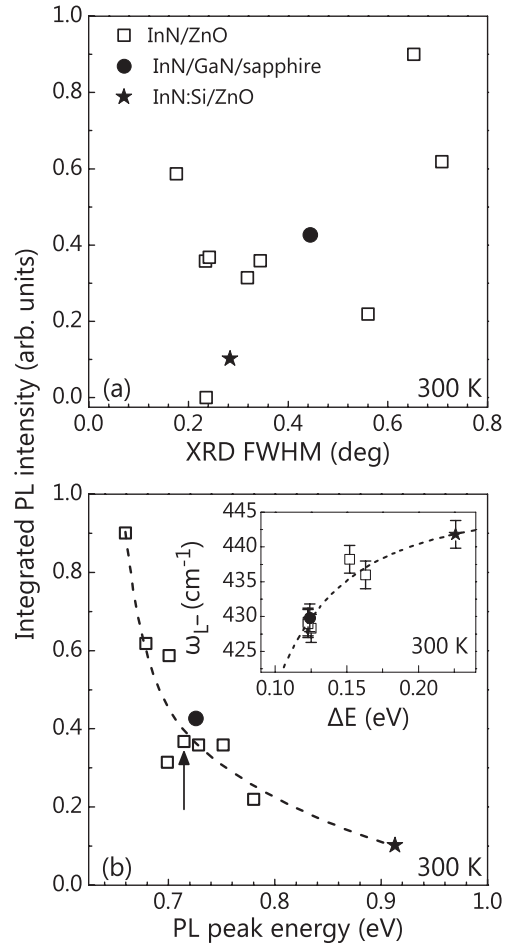


FIG. 2. (a) Integrated PL intensity vs the FWHM of  $(10\bar{1}2)$  XRD  $\omega$  scans for the InN films investigated in this paper. (b) Integrated PL intensity vs PL peak energy ( $E_p$ ) for these InN films. The arrow highlights the InN/ZnO film grown under the same conditions as the Si-doped InN/ZnO film. The dashed line is a guide to the eye. The inset shows the peak frequency of the coupled plasmon/longitudinal-optical-phonon mode  $L^-$  vs  $\Delta E$  for some of the samples. The dashed line is a fit to the data.

In contrast,  $I_{\text{int}}$  is clearly correlated to  $E_p$  as shown in Fig. 2(b), suggesting that the decrease in the PL intensity is, indeed, caused by an increase in electron density. This conclusion is confirmed by a comparison of the two samples grown under the same conditions but being either intentionally undoped or highly doped with Si. In Fig. 2, the intentionally undoped sample is highlighted by an arrow, and its intentionally doped counterpart is represented by an asterisk. Not only is the PL band of the latter sample shifted by about 200 meV to higher energy compared to the former reflecting its much higher electron density, but also its integrated intensity is more than a factor of 3 lower.

$E_p$ , however, is not a very robust measure for  $n$  since its dependence on the Fermi energy is complex and requires an involved line-shape analysis for a quantitative estimate.<sup>18</sup> The inset of Fig. 2(b) displays the relation between two quantities which reflect  $n$  more directly, namely, the frequency of the  $L^-$  mode  $\omega_{L^-}$  and the PL linewidth  $\Delta E$ . Both of these quantities exhibit a simple  $n^{1/2}$  dependence in a certain range of carrier

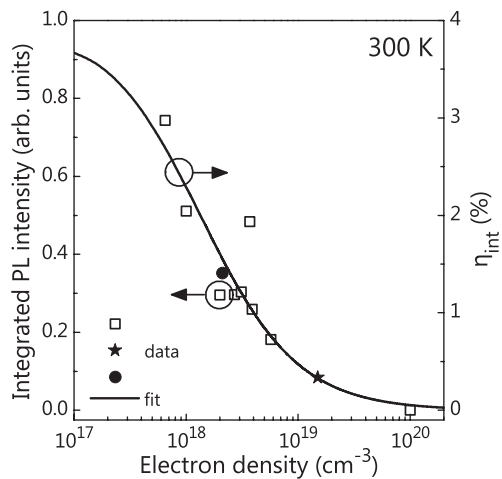


FIG. 3. Integrated PL intensity (symbols) of the InN films investigated in this paper and the internal quantum efficiency  $\eta_{\text{int}}$  vs the electron density for degenerate InN (solid line).

densities. The data points shown in the inset are seen to essentially coincide with the dependence of  $\omega_{L-}$  on electron density<sup>21</sup> (dashed line) taking  $\Delta E \propto \omega_p$ , where  $\omega_p$  is the plasma frequency, which, in turn, is proportional to  $n^{1/2}$ . Both  $\omega_{L-}$  and  $\Delta E$  can, thus, be used for a determination of  $n$ . Since we can measure the former quantity only for our thicker films due to the interference with the  $E_2$  mode of the ZnO substrate, we will use  $\Delta E$  obtained at 10 K (which exhibits a strict  $n^{1/2}$  dependence according to Ref. 17) for the determination of  $n$ .

The experimentally observed decrease in  $I_{\text{int}}$  with an increase in  $n$  points at Auger recombination as being the dominant recombination mechanism for our more highly doped samples. For testing this hypothesis, in Fig. 3, we plot  $I_{\text{int}}$  of the samples under investigation vs  $n$  as determined by the procedure described above. Despite the scatter of the experimental data, this plot evidences that  $I_{\text{int}}$  decreases systematically with increasing  $n$ .

Prior to a quantitative analysis of this dependence, let us point out that we cannot, in principle, rule out that the decrease in  $I_{\text{int}}$  is caused by nonradiative recombination at point defects whose concentration increases proportional to the electron density. However, we do not believe that this potential explanation of our observation, while possible, is a plausible or even probable one. First of all, the electron density in our samples (except for one) is caused by O, which is known to be a substitutional shallow donor in InN even for very high densities.<sup>13</sup> Second, a compensation of these O donors by acceptorlike native point defects is theoretically predicted to be suppressed in InN due to the high formation energies of the native point defects in InN.<sup>14,27</sup> Furthermore, these acceptorlike native defects do not form states in the gap, inhibiting them to act as nonradiative centers unless the electron density is well above  $10^{20} \text{ cm}^{-3}$ .<sup>27</sup> Experimentally, such a generation of point defects at higher concentrations of O would be expected to cause an increasing electrical compensation, thus, limiting the achievable electron density in contrast to the well-known fact that electron densities in excess of  $10^{20} \text{ cm}^{-3}$  can easily be achieved. Third, the intentionally Si-doped sample (see the star-shaped symbol in Fig. 3) follows

the same trend as observed for the unintentionally doped samples. Finally, let us point out that, for the carrier lifetime, Chen *et al.*<sup>28</sup> and Ascázu *et al.*<sup>29</sup> observed the same  $n^{-1}$  dependence as depicted in Fig. 3. Their rejection of Auger recombination as a possible explanation for this finding was based on the (erroneous) assumption that Auger recombination should result in an  $n^{-2}$  dependence of the lifetime. As we will see below, the inverse lifetime resulting from direct Auger recombination in degenerate InN is actually expected to scale linearly with carrier density not quadratically.

The integrated PL intensity is proportional to the internal quantum efficiency  $\eta_{\text{int}}$ , which, in turn, is given by the ratio of the radiative ( $\Gamma_R$ ) and the total ( $\Gamma_T$ ) recombination rate, the latter of which includes nonradiative contributions due to the extrinsic Shockley-Read-Hall (SRH) and the intrinsic Auger mechanisms. In an  $n$ -type semiconductor, the radiative as well as the nonradiative rates are proportional to the photoexcited hole density  $\Delta p$ , and their rate coefficients explicitly depend on both the background doping  $n$  and the photoexcited electron density  $\Delta n$  (which is not, in general, equal to  $\Delta p$  due to the presence of SRH centers).<sup>30</sup> The extraction of the Auger coefficient from high-excitation experiments which aim to vary  $\Delta p$  is, thus, actually more complicated than commonly assumed unless  $\Delta n \gg n$ . However, even when this condition is met, the dependence of the Auger rate on carrier density differs according to the actual Auger mechanism in a given material, and the *a priori* assumption of a cubic dependence for the Auger rate may lead to erroneous conclusions on the relative importance of radiative and Auger contributions.<sup>31,32</sup>

Our experiments are complementary to these high-excitation experiments in that we vary  $n$  instead of  $\Delta p$ . The analysis of our data is greatly simplified for two reasons: First, we employ small-signal excitation with  $\Delta p \ll n$ , and second, we deal with a degenerate semiconductor. In fact, for InN with its low electron mass, degeneracy sets in at electron densities  $n$  of  $2 \times 10^{17} \text{ cm}^{-3}$ , i.e., most InN films available and, certainly, all used in this paper are degenerate. The radiative rate coefficient is then simply given by a rate constant  $B_0$ , having the meaning of an inverse lifetime being independent of  $n$ . Furthermore, the SRH rate coefficient reduces to a rate constant  $T_0$  independent of  $n$  as well, and we can, thus, write

$$\eta_{\text{int}} = \frac{\Gamma_R}{\Gamma_T} = \frac{B_0}{T_0 + B_0 + B_1 n^\beta}, \quad (1)$$

where  $B_1$  represents the Auger rate coefficient with the exponent  $\beta$  depending on the actual Auger mechanism.<sup>33</sup>

Obviously, a determination of  $B_1$  requires the knowledge of both  $T_0$  and  $B_0$ . The latter is equal to the dipole transition rate constant in a dielectric medium and is, thus, easily calculated to be  $2.5 \times 10^8 \text{ s}^{-1}$ .<sup>8</sup> An upper limit of the former can then be derived from the ratio of the integrated PL intensities at low and room temperatures, which we have measured to be 0.04 for InN films with low background doping densities. These numbers result in a SRH rate constant of  $T_0 = 6 \times 10^9 \text{ s}^{-1}$ . Having, thus, acquired a quantitative estimate of the two rate constants  $T_0$  and  $B_0$ , we fit the data with the expression in Eq. (1) and two free parameters, namely,  $B_1$  and  $\beta$ . The fit returns  $\beta \approx 1$  and  $B_1 = (4.5 \pm 2) \times 10^{-9} \text{ cm}^3/\text{s}$ , i.e., the inverse Auger lifetime ( $B_1 n$ ) is, indeed, linear in carrier density, and the rate is quadratic. This specific dependence is expected for the

direct first-order (i.e., neither phonon- nor impurity-assisted) Auger mechanism in degenerate narrow-gap semiconductors, such as InN.<sup>33,34</sup> More recently, fully microscopic many-body calculations have predicted a quadratic dependence for the Auger rate of various other semiconductors, including the wide-gap semiconductor GaN.<sup>31,32</sup>

For comparison with other studies on InN, the Auger rate coefficient  $B_1$  corresponds to an Auger lifetime of 20 ps at an electron density of  $10^{19}$  cm<sup>-3</sup>. Chen *et al.*<sup>28</sup> and Ascáubi *et al.*<sup>29</sup> measured a lifetime of 40 ps for their unintentionally doped InN films with this background doping density by pump-probe experiments. They also observed a clear  $1/n$  dependence of the lifetime for films with background electron densities between  $5 \times 10^{17}$  and  $1 \times 10^{19}$  cm<sup>-3</sup>, and their results are, thus, consistent with Eq. (1) and values for  $B_1$  close to the one derived from the fit displayed in Fig. 3. Comparable lifetimes were also obtained by high-excitation time-resolved PL in the paper of Jang *et al.*,<sup>9</sup> who measured values between 30 and 60 ps for  $\Delta n = 10^{19}$  cm<sup>-3</sup> at 200 K. These authors, however, neglected the degeneracy of the samples under investigation and arrived at comparatively small Auger coefficients in their data analysis. Finally, Tsai *et al.*<sup>8</sup> investigated InN films by pump-probe experiments and observed biexponential transients with a fast and a slow component. They attributed the slow component to carrier

recombination and arrived, in their analysis, at an Auger coefficient of  $B_1 = (2.5 \pm 1) \times 10^{-10}$  cm<sup>3</sup>/s, i.e., more than 1 order of magnitude smaller compared to that obtained in the present paper. The fast component of their transients, however, would correspond to an Auger lifetime identical to ours, namely, about 20 ps at an electron density of  $10^{19}$  cm<sup>-3</sup>.

To conclude, the essential factor which limits the use of InN for applications does not seem to be the fact that it has to be prepared heteroepitaxially and, thus, exhibits a high dislocation density but rather its invariably high background doping density. The high carrier density in conjunction with the large Auger coefficient derived here and in previous papers results in a short carrier lifetime and a low internal quantum efficiency, rendering the material of little use for optoelectronic applications. Advances in vacuum technology as well the improved purity of source materials and precursors have led to a reduction in the background doping of InN to values in the mid- $10^{17}$  cm<sup>-3</sup> for state-of-the-art films, but applications in the areas of light emission and photovoltaics demand a further reduction to values well below  $10^{17}$  cm<sup>-3</sup>.

The authors would like to thank H.-P. Schönherr for the maintenance of the MBE system, A. Fiore for useful discussions, and U. Jahn for a critical reading of the manuscript.

\*Present address: Department of Applied Physics, Eindhoven University of Technology, 5600 MB Eindhoven, The Netherlands.

†brandt@pdi-berlin.de

<sup>1</sup>V. Y. Davydov, A. A. Klochikhin, R. P. Seisyan, V. V. Emtsev, S. V. Ivanov, F. Bechstedt, J. Furthmüller, H. Harima, A. V. Mudryi, J. Adrhold, O. Semchinova, and J. Graul, *Phys. Status Solidi B* **229**, R1 (2002).

<sup>2</sup>J. Wu, W. Walukiewicz, K. M. Yu, J. W. Arger III, E. E. Haller, H. Lu, W. J. Schaff, Y. Saito, and Y. Nanishi, *Appl. Phys. Lett.* **80**, 3967 (2002).

<sup>3</sup>G. Koblmüller, C. S. Gallinat, S. Bernardis, J. S. Speck, G. D. Chern, E. D. Readinger, H. Shen, and M. Wraback, *Appl. Phys. Lett.* **89**, 071902 (2006).

<sup>4</sup>J. Kamimura, K. Kishino, and A. Kikuchi, *Appl. Phys. Lett.* **97**, 141913 (2010).

<sup>5</sup>J. Kamimura, K. Kishino, and A. Kikuchi, *Phys. Status Solidi RRL* **6**, 157 (2012).

<sup>6</sup>A. G. Bhuiyan, K. Sugita, K. Kasashima, A. Hashimoto, A. Yamamoto, and V. Y. Davydov, *Appl. Phys. Lett.* **83**, 4788 (2003).

<sup>7</sup>Y. J. Cho, O. Brandt, M. Korytov, M. Albrecht, V. M. Kaganer, M. Ramsteiner, and H. Riechert, *Appl. Phys. Lett.* **100**, 152105 (2012).

<sup>8</sup>T.-R. Tsai, C.-F. Chang, and S. Gwo, *Appl. Phys. Lett.* **90**, 252111 (2007).

<sup>9</sup>D.-J. Jang, G.-T. Lin, C.-L. Hsiao, L. W. Tu, and M.-E. Lee, *Appl. Phys. Lett.* **92**, 042101 (2008).

<sup>10</sup>Y. D. Jang, T. J. Badcock, D. J. Mowbray, M. S. Skolnick, J. Park, D. Lee, H. Y. Liu, M. Hopkinson, R. A. Hogg, and A. D. Andreev, *Appl. Phys. Lett.* **93**, 101903 (2008).

<sup>11</sup>W. K. Metzger, M. W. Wanlass, R. J. Ellingson, R. K. Ahrenkiel, and J. J. Carapella, *Appl. Phys. Lett.* **79**, 3272 (2001).

<sup>12</sup>D. Vignaud, D. A. Yarekha, J. F. Lampin, M. Zakoune, S. Godey, and F. Mollot, *Appl. Phys. Lett.* **90**, 242104 (2007).

<sup>13</sup>C. Stampfl, C. G. Van de Walle, D. Vogel, P. Krüger, and J. Pollmann, *Phys. Rev. B* **61**, R7846 (2000).

<sup>14</sup>C. G. Van de Walle, J. L. Lyons, and A. Janotti, *Phys. Status Solidi A* **207**, 1024 (2010).

<sup>15</sup>B. Heying, X. H. Wu, S. Keller, Y. Li, D. Kapolnek, B. P. Keller, S. P. DenBaars, and J. S. Speck, *Appl. Phys. Lett.* **68**, 643 (1996).

<sup>16</sup>A. Kasic, E. Valcheva, B. Monemar, H. Lu, and W. J. Schaff, *Phys. Rev. B* **70**, 115217 (2004).

<sup>17</sup>M. Moret, S. Ruffenach, O. Briot, and B. Gil, *Appl. Phys. Lett.* **95**, 031910 (2009).

<sup>18</sup>B. Arnaudov, T. Paskova, P. P. Paskov, B. Magnusson, E. Valcheva, B. Monemar, H. Lu, W. J. Schaff, H. Amano, and I. Akasaki, *Phys. Rev. B* **69**, 115216 (2004).

<sup>19</sup>A. A. Klochikhin, V. Y. Davydov, V. V. Emtsev, A. V. Sakharov, V. A. Kapitonov, B. A. Andreev, H. Lu, and W. J. Schaff, *Phys. Rev. B* **71**, 195207 (2005).

<sup>20</sup>M. Feneberg, J. Däubler, K. Thonke, R. Sauer, P. Schley, and R. Goldhahn, *Phys. Rev. B* **77**, 245207 (2008).

<sup>21</sup>G. Abstreiter, M. Cardona, and A. Pinczuk, in *Light Scattering in Solids IV*, edited by M. Cardona and G. Güntherodt (Springer, Berlin, 1984), p. 5.

<sup>22</sup>V. Y. Davydov, V. V. Emtsev, I. N. Goncharuk, A. N. Smirnov, V. D. Petrikov, V. V. Mamutin, V. A. Vekshin, and S. V. Ivanov, *Appl. Phys. Lett.* **75**, 3297 (1999).

<sup>23</sup>R. Cuscó, J. Ibáñez, E. Alarcón-Lladó, L. Artús, T. Yamaguchi, and Y. Nanishi, *Phys. Rev. B* **79**, 155210 (2009).

<sup>24</sup>The intense peak for the thinnest InN films may contain a contribution from the  $E_2$  mode ( $\approx 440$  cm<sup>-1</sup>) of the ZnO substrate.

- <sup>25</sup>L. F. J. Piper, T. D. Veal, C. F. McConville, L. Hai, and W. J. Schaff, *Appl. Phys. Lett.* **88**, 252109 (2006).
- <sup>26</sup>T. Akagi, K. Kosaka, S. Harui, D. Muto, H. Naoi, T. Araki, and Y. Nanishi, *J. Electron. Mater.* **37**, 603 (2008).
- <sup>27</sup>A. Janotti, J. L. Lyons, and C. G. Van de Walle, *Phys. Status Solidi A* **209**, 65 (2012).
- <sup>28</sup>F. Chen, A. N. Cartwright, H. Lu, and W. J. Schaff, *Phys. Status Solidi A* **202**, 768 (2005).
- <sup>29</sup>R. Ascázubi, I. Wilke, S. Cho, H. Lu, and W. J. Schaff, *Appl. Phys. Lett.* **88**, 112111 (2006).
- <sup>30</sup>O. Brandt, H. Yang, and K. H. Ploog, *Phys. Rev. B* **54**, R5215 (1996).
- <sup>31</sup>J. Hader, J. V. Moloney, and S. W. Koch, *Appl. Phys. Lett.* **87**, 201112 (2005).
- <sup>32</sup>J. Hader, J. V. Moloney, B. Pasenow, S. W. Koch, M. Sabathil, N. Linder, and S. Lutgen, *Appl. Phys. Lett.* **92**, 261103 (2008).
- <sup>33</sup>A. Haug, *Solid-State Electron.* **21**, 1281 (1978).
- <sup>34</sup>See, in particular, Eq. (A3) in A. Haug, *Solid State Commun.* **22**, 537 (1977).